EPJ manuscript No.
(will be inserted by the editor)

Status of the N^* Program at Jefferson Lab

Volker D. Burkert

Jefferson Lab, 12000 Jefferson Avenue, Newport News, VA23606

Abstract. Recent results in electromagnetic excitation of nucleon resonance are presented, and confronted with theoretical predictions. Preliminary data in the search for missing states are discussed as well.

PACS. 1 3.60.le, 13.88.+e

1 Introduction

Resonance electroproduction has rich applications in nucleon structure studies at intermediate and large distances. Resonances play an important role in understanding the spin structure of the nucleon [1,2]. More than 80% of the helicity-dependent integrated total photoabsorption cross section difference (GDH integral) is a result of the excitation of the $\Delta(1232)$ [1,3]. At Q^2= 1 GeV^2 about 40% of the first moment $\Gamma_1^P(Q^2) = \int_0^1 g_1(x,Q^2)dx$ for the proton is due to contributions of the resonance region at $W < 2$GeV [4–6]. Conclusions regarding the nucleon spin structure for $Q^2 < 2$ GeV^2 must therefore be regarded with some scepticism if contributions of baryon resonances are not taken into account.

The nucleon's excitation spectrum has been explored mostly with pion beams. Many states, predicted in the standard quark model, have not been seen in these studies, possibly many of them decouple from the $N\pi$ channel [7]. Electromagnetic interaction and measurement of multi-pion final states may then be the only way to study some of these states. While photoproduction is one way, electroproduction, though harder to measure, adds additional sensitivity due to the possibility of varying the photon virtuality.

Electroexcitation in the past was not considered a tool of baryon spectroscopy. CLAS is the first full acceptance instrument with sufficient resolution to measure exclusive electroproduction of mesons with the goal of studying the excitation of nucleon resonances in detail. The entire resonance mass region, a large range in the photon virtuality Q^2 can be studied, and many meson final states are measured simultaneously. Figure 1 shows the coverage in the invariant hadronic mass W and the missing mass M_X for the process $ep \to epX$ for a 4 GeV electron beam.

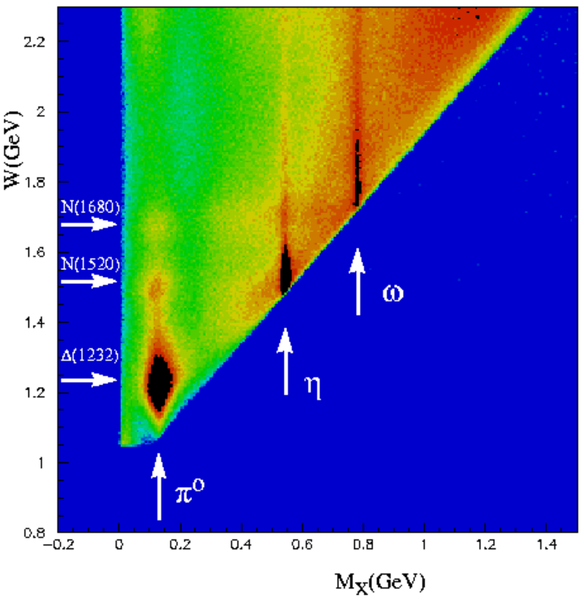

Fig. 1. Hadronic invariant mass W versus missing mass M_X for $\gamma^* p \to pX$, measured in CLAS. The vertical arrows indicate bands of π°, η, and ω mesons. The horizontal arrows mark the masses of several resonances.

2 Quadrupole deformation of the $\Delta(1232)$ and QCD

An interesting aspects of nucleon structure at low energies is a possible quadrupole deformation of the nucleon or its lowest excited state. In the interpretation of ref. [8] this would be evident in non-zero values of the quadrupole transition amplitudes E_{1+} and S_{1+} from the nucleon to the $\Delta(1232)$. In models with $SU(6)$ spherical symmetry, this transition is simply due to a magnetic dipole M_{1+} mediated by a spin flip from the $J = \frac{1}{2}$ nucleon ground state to the Δ with $J = \frac{3}{2}$, giving $E_{1+} = S_{1+} = 0$. Non-zero values for E_{1+} and S_{1+} would indicate deformation. Dynamically such deformation may arise through

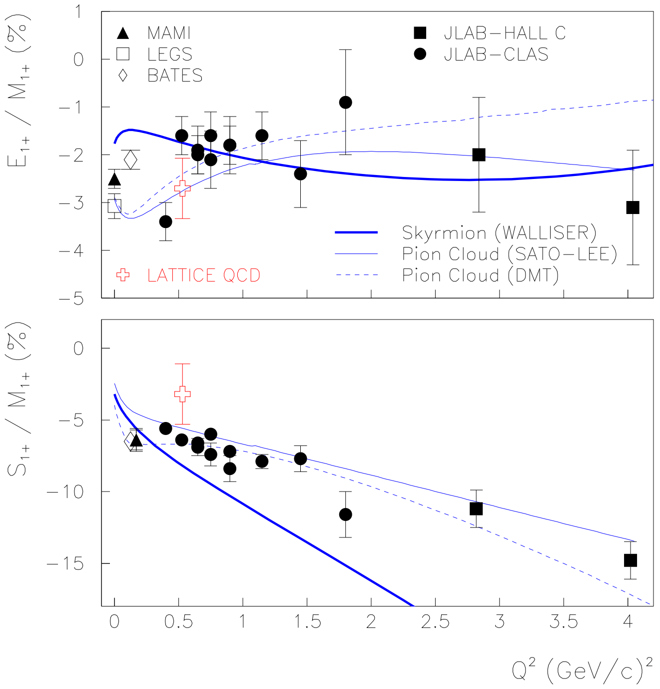

Fig. 2. R_{EM} and R_{SM} after 1990, including the recent CLAS results[14] and the data from Hall-C[17]. It also shows the recent Lattice QCD points.

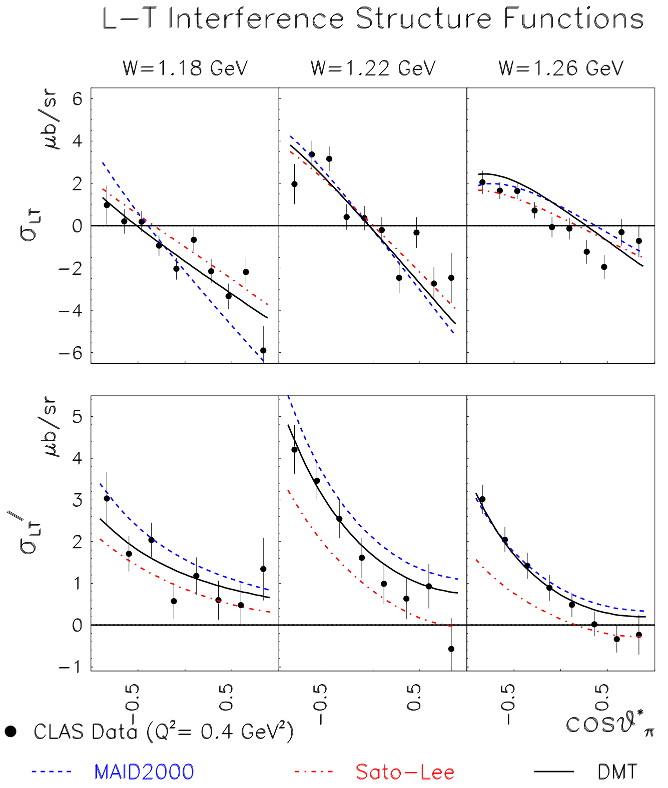

Fig. 3. Data on σ_{LT}, and preliminary $\sigma_{LT'}$ data from CLAS compared to predictions of three dynamical models[9–11]. The latter data show strong sensitivity to the non-resonant contributions in the various models.

interaction of the photon with the pion cloud[10,11] or through the one-gluon exchange mechanism [7]. At asymptotic momentum transfer, a model-independent prediction of helicity conservation requires $R_{EM} \equiv E_{1+}/M_{1+} \to +1$. An interpretation of R_{EM} in terms of a quadrupole deformation can therefore only be valid at low momentum transfer.

Results of the multipole analysis of the CLAS data[14] are shown in Fig.2, where data from previous experiments published after 1990 are included as well [15–17]. R_{EM} remains negative and small throughout the Q^2 range. There are no indications that leading pQCD contributions are important as they would result in a rise of $R_{EM} \to +1$ [18]. R_{SM} behaves quite differently. While it also remains negative, its magnitude is strongly rising with Q^2. The comparison with microscopic models, from relativized quark models[19,20], the chiral quark soliton model[21], and dynamical models[10–12] show that simultaneous description of both R_{EM} and R_{SM} is achieved by dynamical models that include the nucleon pion cloud, explicitly. This supports the claim that most of the quadrupole strength is due to meson effects which are not included in other models.

Ultimately, we want to come to a QCD description of these important nucleon structure quantities. At the time of this conference no lattice QCD calculations with sufficient accuracy were available to predict non-zero values for R_{EM}. This situation has changed very recently with a calculation of the R_{EM} and R_{SM} ratio in quenched and unquenched QCD in the Q^2 range of the CLAS results[13]. The full QCD results give R_{EM} values more negative than in the quenched approximation showing the contribution of the pion cloud to be negative, and causing an oblate deformation of the $\Delta(1232)$. The calculation at $Q^2 = 0.52$ GeV^2 is in agreement with the CLAS data for R_{EM} and R_{SM}.

While the new JLab data establish a new level of accuracy, improvements in statistics and the coverage of a larger Q^2 range are expected for the near future, and they must be complemented by a reduction of model dependencies in the analysis. This becomes increasingly important as the full QCD calculations get more precise, and calculations in a wide range of Q^2 may be forthcoming. It would be highly interesting to see if QCD calculations can describe the observed Q^2 evolution of R_{SM}.

Model dependencies in the analysis are largely due to our poor knowledge of the non-resonant terms, which become increasingly important at higher Q^2. The $\sigma_{LT'}$ response function, a longitudinal/transverse interference term is especially sensitive to non-resonant contributions if a strong resonance is present. $\sigma_{LT'}$ can be measured using a polarized electron beam in out-of-plane kinematics for the pion. Preliminary data on $\sigma_{LT'}$ from CLAS are shown in Fig. 3 in comparison with dynamical models, clearly showing the model sensitivity to non-resonant contributions. All models predict nearly the same unpolarized cross sections at the Δ mass (upper panel for W = 1.22 GeV), however they differ in their handling of non-resonant contributions.

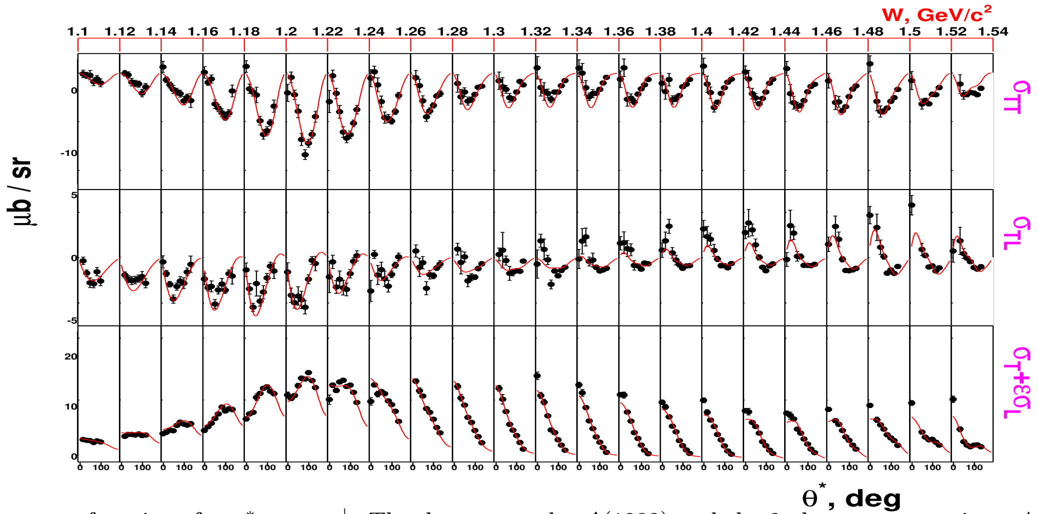

Fig. 4. Response functions for $\gamma^* p \to n\pi^+$. The data cover the $\Delta(1232)$ and the 2nd resonance regions. Angular distributions are show for each bin in W. The data provide the basis for the analysis with a unitary isobar model[26].

3 N^*'s in the second resonance region

Three states, the "Roper" $N'_{1/2^+}(1440)$, and two strong negative parity states, $N^*_{3/2^-}(1520)$, and $N^*_{1/2^-}(1535)$ make up the second enhancement seen in inclusive electron scattering. All of these states are of special interest to obtain a better understanding of nucleon structure and strong QCD.

3.1 The Roper resonance - still a mystery

The Roper resonance has been a focus of attention for the last decade, largely due to the inability of the standard constituent quark model to describe basic features such as the mass, photocouplings, and their Q^2 evolution. This has led to alternate approaches where the state is assumed to have a strong gluonic component [22], a small quark core with a large meson cloud [23], or a hadronic molecule of a nucleon and a hypothetical σ meson $|N\sigma>$ [24]. Lattice QCD calculations [28] show no sign of a 3-quark state with the quantum numbers of the nucleon in the mass range of the Roper state. The lowest excited 3-quark state with the quantum numbers of the nucleon may be predicted in a mass range above 2 GeV. Given this result the question of what is the nature of the existing Roper state becomes an urgent topic to address. Electroexcitation may help provide an answer as it probes the underlying structure.

The Roper, as an isospin 1/2 state, couples more strongly to the nπ^+ channel than to the pπ^o channel. Lack of data in that channel and lack of polarization data has hampered progress in the past. Fortunately, this sitation is changing significantly with the new data from CLAS. For the first time complete angular distributions have been measured for the nπ^+ final state. Preliminary separated response functions obtained with CLAS[25] are shown in Fig.4. These data, together with the $p\pi^o$ response functions and the spin polarized $\sigma_{LT'}$ response function for both channels, have been fitted to a unitary isobar model[26]. The results are shown in Fig. 5 together with the sparse data from previous analyses. The CLAS results confirm the fast fall-off with Q^2 for the $A_{1/2}$ amplitude. Much improved data are needed for more definite tests of the models in a larger Q^2 range. An interesting question is whether the $A_{1/2}(Q^2)$ amplitude changes sign, or remains negative. The range of model predictions for the Q^2 evolution illustrates dramatically the sensitivity of electroproduction to the internal structure of this state.

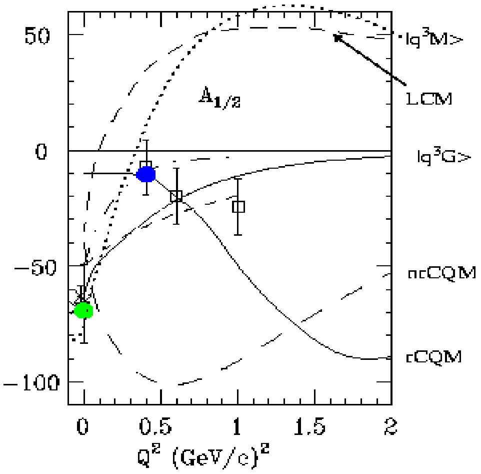

Fig. 5. Transverse helicity amplitude $A_{1/2}(Q^2)$ for the Roper resonance. The full (blue) circle shows preliminary results of an analysis of CLAS data at $Q^2 = 0.4\mathrm{GeV}^2$. The curves represent model predictions.

3.2 The first negative parity state $N^*_{1/2^-}(1535)$

Another state of special interest in the 2nd resonance region is the $N^*_{1/2^-}(1535)$. This state was found to have an unusually hard transition formfactor, i.e. the Q^2 evolution shows a slow fall-off. This state is often studied in the $p\eta$ channel which shows a strong s-wave resonance near the η-threshold with very little non-resonant background. Older data show some discrepancies as to the total width and photocoupling amplitude. In particular, analyses of pion photoproduction data[42] disagree with the analysis of the η photoproduction data by a wide margin.

Data from CLAS[29], together with data from an earlier JLab experiment[30] now give a consistent picture of the Q^2 evolution, confirming the hard formfactor behavior with much improved data quality, as shown in Fig. 6. Analysis of the nπ^+ and pπ^o data at Q^2= 0.4GeV^2 gives a value for $A_{1/2} \approx 105 \times 10^{-3}$ GeV$^{-1/2}$ consistent with the analysis of the pη data[31].

The hard transition formfactor has been difficult to understand in models. Recent work within a constituent quark model using a hypercentral potential [32] has made progress in reproducing the transition amplitude $A_{1/2}$ to the $N^*_{1/2^-}(1535)$. The hard formfactor is also in contrast to models that interpret this state as a $|\bar{K}\Sigma >$ hadronic molecule [27]. Although no calculations exist from such models, the extreme "hardness" of the formfactor and the large cross section appear counter intuitive to an interpretation of this state as a bound hadronic system. Lattice QCD calculations also show very clear 3-quark strength for the state [28].

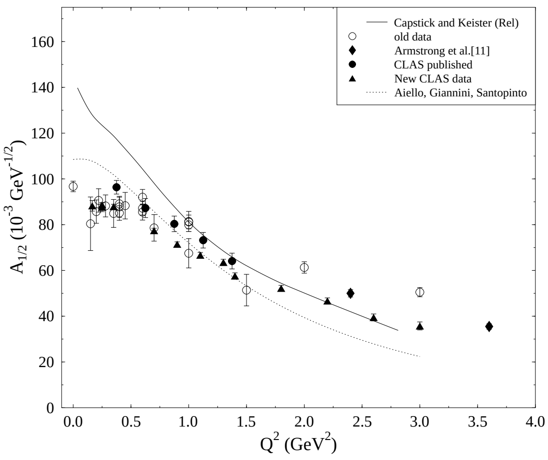

Fig. 6. Transverse helicity amplitude $A_{1/2}(Q^2)$ for the first negative parity state $N^*_{1/2^-}(1535)$.

4 Higher mass states and missing resonances

Approximate $SU(6) \otimes O(3)$ symmetry of the symmetric constituent quark model leads to relationships between the various states. In the single-quark transition model (SQTM) only one quark participates in the interaction. The model predicts transition amplitudes for a large number of states based on only a few measured amplitudes [35]. Comparison with photoproduction results show quite good agreement, while there are insufficient electroproduction data for a meaningful comparison. The main reason is that many of the higher mass states decouple largely from the $N\pi$ channel, but couple dominantly to the $N\pi\pi$ channel. Study of $\gamma^* p \to p\pi^+\pi^-$ as well as the other charge channels are therefore important. Moreover, many of the so-called "missing" states are predicted to couple strongly to the $N\pi\pi$ channels [39]. Search for some of these states is of great importance for the understanding of nucleon structure as alternative symmetry schemes do not predict nearly as many "missing" states[36].

4.1 Resonances in the $p\pi^+\pi^-$ channel.

New CLAS total cross section electroproduction data are shown in Fig. 7 in comparison with photoproduction data from DESY [37]. The most striking feature is the strong resonance peak near W=1.72 GeV seen for the first time in electroproduction of the $p\pi^+\pi^-$ channel. This peak is absent in the photoproduction data. The CLAS data [38] also contain the complete hadronic angular distributions and $p\pi^+$ and $\pi^+\pi^-$ mass distributions over the full W range. They have been analyzed and the peak near 1.72 GeV was found to be best described by a $N^*_{3/2^+}(1720)$ state. While there exists a state with such quantum numbers in this mass range, its hadronic properties were found previously to be very different from the state observed in this experiment. The difficulties in decribing these results seems to rest with the hadronic properties of the PDG state. Trying to keep the couplings within the limits of analyses of hadronic processes forces a strong reduction of the electrocouplings and the introducion of a second state with the same quantum numbers but strongly different hadronic couplings (solid line).

Could this state be one of the "missing" states? Capstick and Roberts [39] predict a second $N^*_{3/2^+}$ state at a mass 1.87GeV. There are also predictions of a hybrid baryon state with these quantum numbers at about the same mass [41], although the rather hard form factor disfavors the hybrid baryon interpretation [22]. As mass predictions in these models are uncertain to at least $\pm$100MeV, interpretation of this state as a "missing" state is a definite possibility. Independent of possible interpretations, the hadronic properties of the state seen in the CLAS data appear incompatible with the properties of the known state with same quantum numbers as listed in Review of Particle Properties [42] and the analyses of $N\pi\pi$ final states in πN scattering.

4.2 Nucleon states in $K\Lambda$ production?

Strangeness channels have recently been examined in photoproduction as a possible source of information on new

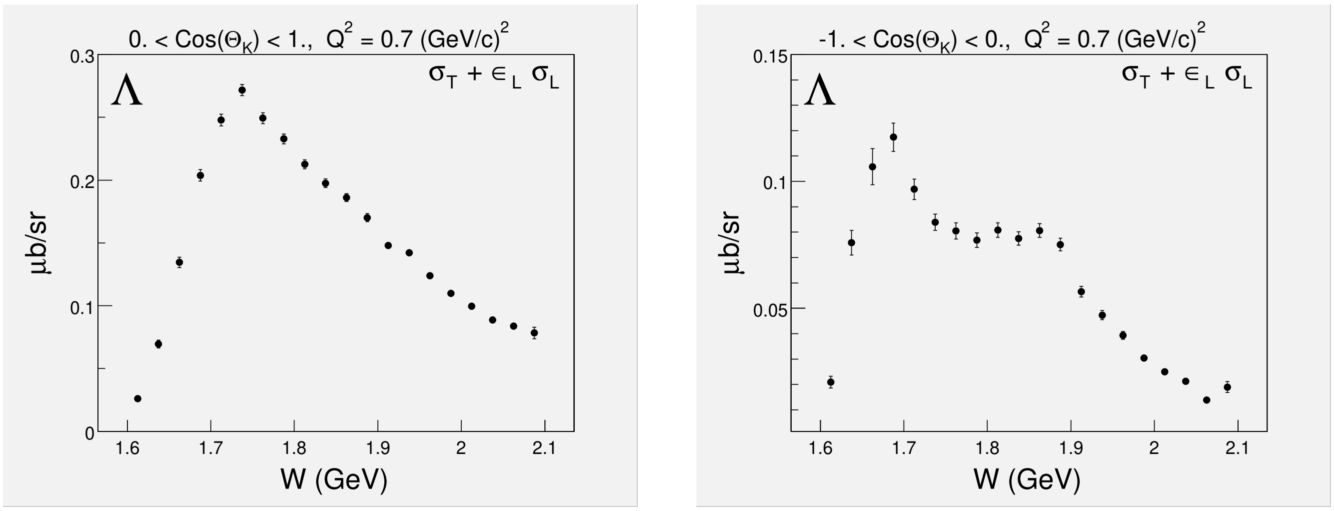

Fig. 8. Total photoabsorption cross section measured with CLAS for $\gamma^* p \rightarrow K^+ \Lambda$. The left panel is integrated over the full forward hemisphere in the K^+ angular distribution in the $K^+\Lambda$ cms. The right panel is integrated over the backward hemisphere .

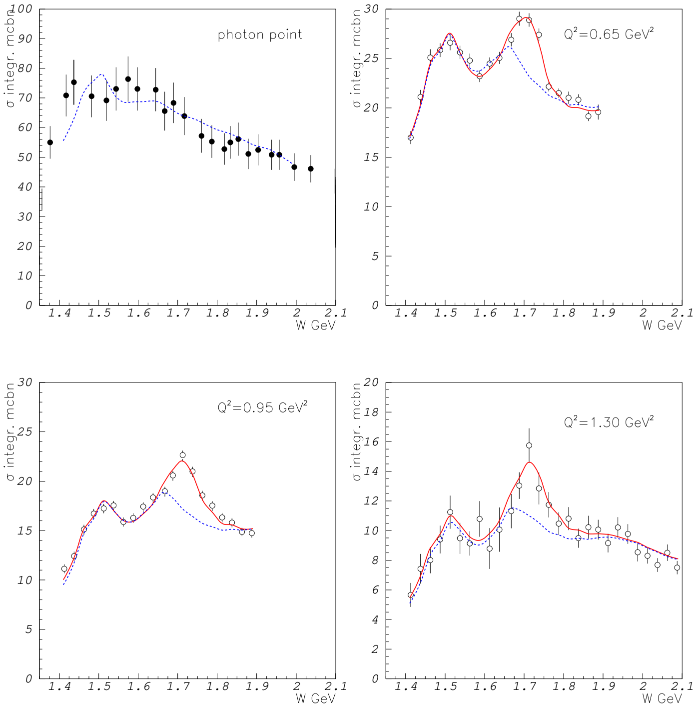

Fig. 7. Total photoabsorption cross section for $\gamma^* p \rightarrow p\pi^+\pi^-$. Photoproduction data from DESY - top left panel. The other panels show CLAS electroproduction data at $Q^2 = 0.65,\ 0.95,\ 1.3\ \mathrm{GeV}^2$. The resonance structure near 1.7 GeV is emerging with increasing Q^2. The dashed lines represents our knowledge of N^* electromagnetic and hadronic properties with the couplings varied within empirical uncertainties. The solid line is a best fit to the data assuming the existence of a second $N^*_{3/2^+}(1720)$ with different hadronic couplings.

baryon states, and candidate states have been discussed [33,34]. New CLAS electroproduction data [45] in the $K\Lambda$ channel show clear evidence for resonance excitations at masses of 1.7 and 1.85 GeV as show in Fig. 8. The analysis of the $K\Lambda$ channel is somewhat complicated by the large t-channel exchange contribution producing a peak at forward angles. To increase sensitivity to s-channel processes the data have been divided into a set for the forward hemisphere and for the backward hemisphere. Clear structures in the invariant mass emerge for the backward hemisphere (right panel in Fig. 8). While the lower mass peak is probably due to known resonances, the peak near 1.85 GeV could be associated with the bump observed with the SAPHIR detector [33], although its mass seems to be lower. A more complete analysis of the angular distribution and the energy-dependence is needed for more definite conclusions.

4.3 Photoproduction of η mesons

New results on $\gamma p \rightarrow p\eta$ have recently become available from CLAS[43] covering the resonance region for $W < 2.15$ GeV. Nearly complete angular distributions have been measured and the total cross section has been extracted. The total cross section data are shown in Figure 9. The data show structure beyond the well known $N^*(1535)$ indicative of higher mass resonance contributions to the $p\eta$ channel. Further analysis of the angular and energy dependences are needed to come to more definite conclusions on the excitation of specific resonances.

4.4 Resonances in virtual Compton scattering

Vitual Compton scattering, i.e. the process $\gamma^* p \rightarrow p\gamma$ is yet another tool in the study of excited baryon states.

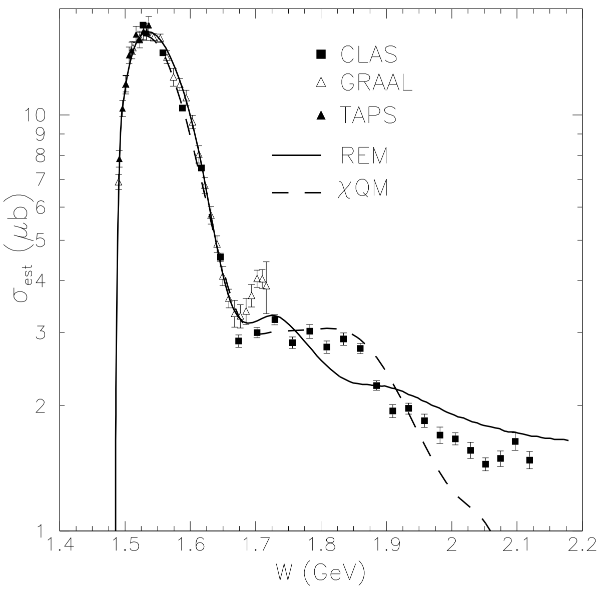

Fig. 9. Total η photoproduction cross sections from protons.

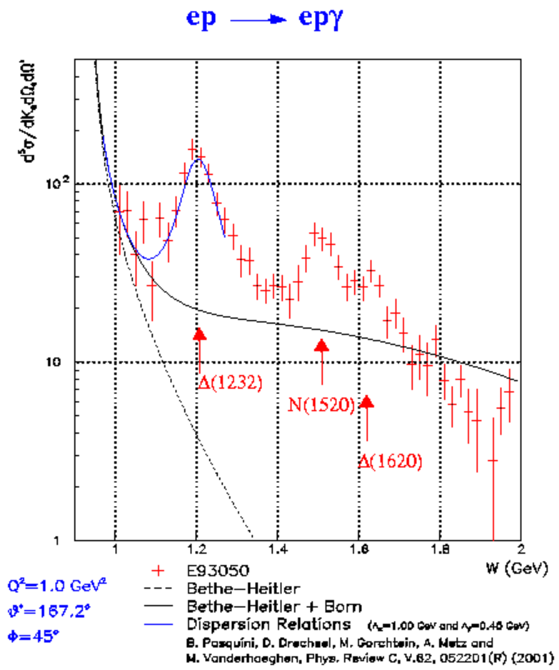

Fig. 10. Differential cross section for virtual Compton scattering at $Q^2 = 1$ GeV^2. The final state photon is in the backward direction relative to the virtual photon.

This process has recently been measured in experiment E93-050 in JLab Hall A[44] at backward proton angles. The excitation spectrum shown in Fig.10 exhibits clear resonance excitations at masses of known states such as the $\Delta(1232)$, $N^*(1520)$, and $N^*(1650)$. The attractive feature of this process is the absence of final state interaction which complicates the analysis of processes with mesons in the final state. The disadvantage is the low rate which makes it difficult to collect sufficient statistics for a full partial wave analysis.

5 Baryon spectroscopy at short distances

Inelastic virtual Compton scattering in the deep inelastic regime (DVSC) can provide a new avenue of resonance studies at the elementary quark level. The process of interest is $\gamma^* p \rightarrow \gamma N^*(\Delta^*)$ where the virtual photon has high virtuality (Q^2). The virtual photon couples to an elementary quark with longitudinal momentum fraction x, which is re-absorbed into the baryonic system with momentum fraction $x - \xi$, after having emitted a high energy photon. The recoil baryon system may be a ground state proton or an excited state. The elastic DVCS process has recently been measured at JLab [46] and at DESY [47] in polarized electron proton scattering, and the results are consistent with predictions from perturbative QCD and the twist expansion for the process computed at the quark-gluon level. The theory is under control for small momentum transfer to the final state baryon. For the inelastic process, where a N^* or Δ resonance is excited, the process can be used to study resonance transitions at the elementary quark level. Varying the parameter ξ and the momentum transfer to the recoil baryon probes the two-parton correlation functions, or generalized parton distributions (GPDs).

That this process is indeed present at a measureable level is seen in the preliminary data from CLAS [48] shown in Fig. 11. The reaction is measured at invariant masses $W > 2$ GeV. The recoiling baryonic system clearly shows the excitation of resonances, the $\Delta(1232)$, $N^*(1520)$, and $N^*(1680)$. While these are well known states that are also excited in the usual s-channel processes, the DVCS process has the advantage that it decouples the photon virtuality Q^2 from the 4-momentum transfer to the baryon system. Q^2 may be chosen sufficiently high such that the virtual photon couples to an elementary quark, while the momentum transfer to the nucleon system can be varied independently from small to large values. In this way, a theoretical framework employing perturbative methods can be used to probe the "soft" NN^* transition, allowing to map out internal parton correlations for this transition.

6 Conclusions

Electroexcitation of nucleon resonances has evolved to an effective tool in studying nucleon structure in the regime of strong QCD and confinement. The new data from JLab in the $\Delta_{3/2^+}(1232)$ and $N^*_{1/2^-}(1535)$ regions give a consistent picture of the Q^2 evolution of the transition form factors. The R_{EM} and R_{SM} ratios for the $\gamma^* N\Delta(1232)$ transition are consistent with an oblate deformation of the Δ^+. This is now also confirmed by calculations in full lattice QCD. Large data sets in different channels including polarization observables will vastly improve the analysis of states such as the "Roper" $N'_{1/2^+}(1440)$, and many other

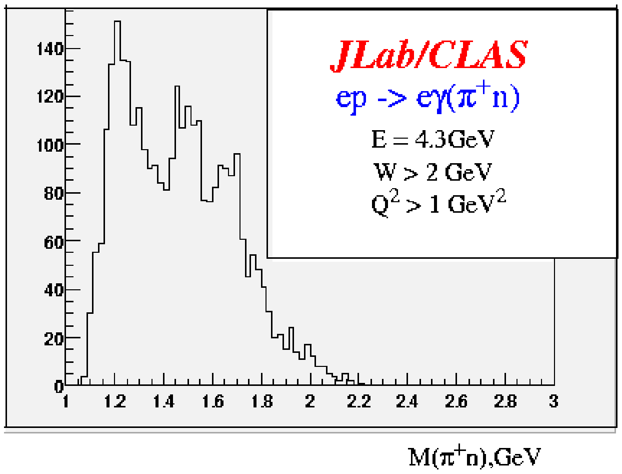

Fig. 11. Inelastic deeply virtual Compton scattering measured in CLAS. The recoiling $(n\pi^+)$ system clearly shows the excitation of several resonances, the $\Delta(1232)$, $N^*(1520)$, and $N^*(1680)$.

higher mass states. A preliminary analysis of $n\pi^+$ and $p\pi^\circ$ cross section data and beam polarization asymmetries at $Q^2 = 0.4$ GeV^2 show little indication of the $N'_{1/2^+}(1440)$, which is consistent with earlier analyses showing a fast drop of the Roper excitation strength with Q^2. A strong resonance signal near 1.72 GeV, seen with CLAS in the $p\pi^+\pi^-$ channel, exhibits hadronic properties which appear incompatible with any of the known states in this mass region and may indicate a new $N^*_{3/2^+}(1720)$ state.

While s-channel resonance excitation will remain the backbone of the N^* program for years to come, inelastic deeply virtual Compton scattering is a promising new tool in resonance physics at the elementary parton level that allows the study of parton-parton correlations in resonance transition within a well defined theoretical framework.

The Southeastern Universities Research Association (SURA) operates the the Thomas Jefferson National Accelerator Facility for the United States Department of Energy under Contract No. DE-AC05-84ER40150.

References

1. V.D. Burkert, and Zh. Li, Phys. Rev. D47:46-50, 1993.
2. V.D. Burkert and B.L. Ioffe, Phys. Lett. B296:223-226, 1992; J.Exp.Theor.Phys.78:619-622, 1994.
3. J. Ahrens et al., Phys.Rev.Lett. 87:022003, 2001.
4. R. De Vita, talk at BARYONS2002, to appear in the proceedings,eds. C. Carlson, B. Mecking.
5. V.D. Burkert, Nucl.Phys.A699:261-269, 2002.
6. R. Minehart, talk at NSTAR 2001, World Scientific, eds. D. Drechsel, L. Tiator.
7. R. Koniuk and N. Isgur, Phys.Rev.D21:1868, 1980.
8. A. Buchmann and E. Henley, Phys.Rev.D65:073017, 2002.
9. D. Drechsel, O. Hanstein, S.S. Kamalov, L. Tiator, Nucl.Phys.A645, 145, 1999.
10. T. Sato and T.S. Lee, Phys.Rev.C63, 055201, 2001.
11. S.S. Kamalov and S.N. Yang, Phys.Rev.Lett.83:4494-4497, 1999.
12. S.S. Kamalov et al., Phys.Rev.C64,033201, 2001.
13. C. Alexandrou et al., hep-lat/0209074, 2002.
14. K. Joo, et al, Phys.Rev.Lett.88, 122001, 2002.
15. R. Beck et al., Phys.Rev.C61:035204, 2000.
16. G. Blanpied et al., Phys.Rev.C64:025203, 2001.
17. V.V. Frolov et al., Phys.Rev.Lett.82:45-48, 1999.
18. G. A. Warren, C.E. Carlson, Phys.Rev.D42:3020-3024, 1990.
19. M. Warns, H. Schroder, W. Pfeil, H. Rollnik, Z.Phys.C45:627, 1990
20. I.G. Aznaurian, Z.Phys.A346:297-305, 1993.
21. A. Silva et al., Nucl.Phys.A675:637-657, 2000.
22. Z.P. Li, V. Burkert, Zh. Li; Phys.Rev.D46, 70, 1992.
23. F. Cano and P. Gonzales, Phys.Lett.B431:270-276, 1998.
24. O. Krehl, C. Hanhart, S. Krewald, J. Speth, Phys.Rev.C62:025207, 2000.
25. H. Egiyan at al., to be submitted to Phys.Rev.C.
26. I. Aznauryan, nucl-th/0206033, 2002.
27. N. Kaiser, P.B. Siegel, W. Weise, Phys.Lett.B362, 23, 1995.
28. S. Sasaki, T. Blum, S. Ohta Phys.Rev.D65:074503.
29. R. Thompson et al., Phys.Rev.Lett.86, 1702, 2001, H. Denizli, private communications.
30. C.S. Armstrong et al., Phys.Rev.D60:052004, 1999.
31. I. Aznaurian et al., to be submitted to Phys.Rev.C.
32. M.M. Giannini, E. Santopinto, A. Vassallo, Nucl.Phys.A699, 308, 2002.
33. M.Q. Tran et al., Phys.Lett.B445:20-26, 1998.
34. A. d'Angelo, talk at BARYONS 2002, to appear in the proceedings, eds. C. Carlson, B. Mecking.
35. W.N. Cottingham and I.H. Dunbar, Z.Phys.C2, 41, 1979.
36. M. Kirchbach. Mod.Phys.Lett.A12:3177-3188, 1997.
37. V. Eckart et al., Nucl.Phys.B55, 45, 1973; P. Joos et al., Phys.Lett.B52, 481, 1974; K. Wacker et al., Nucl.Phys.B144, 269, 1978.
38. M. Ripani, Nucl.Phys.A699:270-277, 2002.
39. S. Capstick and W. Roberts, Phys.Rev.D49:4570-4586, 1994.
40. V.I. Mokeev, et al., Phys.Atom.Nucl.64:1292-1298, 2001.
41. S. Capstick, P.R. Page, Phys.Rev.D60:111501, 1999.
42. D.E. Groom et al., Eur.Phys.J.C15, 1-878, 2000.
43. M. Dugger, et al., (CLAS collaboration) submitted to Phys. Rev. Lett.
44. H. Fonvieille, talk at BARYONS2002, to appear in the proceedings.
45. G. Niculescu, R. Feuerbach, private communications.
46. S. Stepanyan et al., Phys.Rev.Lett.87, 182002-1, 2001.
47. A. Airapetian et al., Phys.Rev.Lett.87, 182001-1, 2001.
48. M. Guidal, private communications, 2002.